C-terminal phosphorylation regulates the kinetics of a subset of melanopsin-mediated behaviors in mice

Preethi Somasundaram[a], Glenn R. Wyrick[b], Diego Carlos Fernandez[c], Alireza Ghahari[d], Cindy M. Pinhal[b], Melissa Simmonds Richardson[c], Alan C. Rupp[c], Lihong Cui[e], Zhijian Wu[f], R. Lane Brown[b], Tudor Constantin Badea[d], Samer Hattar[c,g,1,2], and Phyllis R. Robinson[a,1]

[a]Department of Biological Sciences, University of Maryland, Baltimore County, Baltimore, MD 21250; [b]Department of Integrative Physiology & Neuroscience, Washington State University, Pullman, WA 99164; [c]Department of Biology, Johns Hopkins University, Baltimore, MD 21218; [d]Retinal Circuit Development & Genetics Unit, Neurobiology Neurodegeneration & Repair Laboratory, National Eye Institute, National Institutes of Health, Bethesda, MD 20892; [e]Genetic Epidemiology Research Branch, National Institute of Mental Health, Bethesda, MD 20892; [f]Ocular Gene Therapy Core, National Eye Institute, National Institutes of Health, Bethesda, MD 20892; and [g]Department of Neuroscience, The Johns Hopkins University School of Medicine, Baltimore, MD 21218

Edited by Joseph S. Takahashi, Howard Hughes Medical Institute, University of Texas Southwestern Medical Center, Dallas, TX, and approved January 24, 2017 (received for review July 19, 2016)

Intrinsically photosensitive retinal ganglion cells (ipRGCs) express the photopigment melanopsin and mediate several non–image-forming visual functions, including circadian photoentrainment and the pupillary light reflex (PLR). ipRGCs act as autonomous photoreceptors via the intrinsic melanopsin-based phototransduction pathway and as a relay for rod/cone input via synaptically driven responses. Under low light intensities, where only synaptically driven rod/cone input activates ipRGCs, the duration of the ipRGC response will be determined by the termination kinetics of the rod/cone circuits. Little is known, however, about the termination kinetics of the intrinsic melanopsin-based phototransduction pathway and its contribution to several melanopsin-mediated behaviors. Here, we show that C-terminal phosphorylation of melanopsin determines the recovery kinetics of the intrinsic melanopsin-based photoresponse in ipRGCs, the duration of the PLR, and the speed of reentrainment. In contrast, circadian phase alignment and direct effects of light on activity (masking) are not influenced by C-terminal phosphorylation of melanopsin. Electrophysiological measurements demonstrate that expression of a virally encoded melanopsin lacking all C-terminal phosphorylation sites (C terminus phosphonull) leads to a prolonged intrinsic light response. In addition, mice expressing the C terminus phosphonull in ipRGCs reentrain faster to a delayed light/dark cycle compared with mice expressing virally encoded WT melanopsin; however, the phase angle of entrainment and masking were indistinguishable. Importantly, a sustained PLR in the phosphonull animals is only observed at brighter light intensities that activate melanopsin phototransduction, but not at dimmer light intensities that activate only the rod/cone pathway. Taken together, our results highlight how the kinetics of the melanopsin photoresponse differentially regulate distinct light-mediated behaviors.

ipRGCs | photoentrainment | photoreceptors | phosphorylation | phototransduction

In addition to detecting light for image-forming vision, the mammalian retina detects light for several non–image-forming visual functions, including photoentrainment of the circadian clock and regulation of pupil size, sleep, and mood. It has been shown recently that these non–image-forming visual functions require a subset of retinal ganglion cells that express the photopigment melanopsin (Opn4), a G protein-coupled receptor (GPCR) (1–3), and are known as intrinsically photosensitive retinal ganglion cells (ipRGCs) (4–6). Recent work has revealed a surprising diversity in ipRGCs, which are now known to comprise at least five distinct subtypes (M1–M5), based on molecular, morphological, and electrophysiological criteria and projection patterns (7). The ipRGCs are unique in that they can respond to light via two independent pathways: First, they can incorporate rod/cone input through classical retinal circuits; alternatively, they can respond intrinsically through melanopsin-based phototransduction machinery (8–12), which can extend many seconds beyond the actual light stimulus. Unlike the light responses of rods and cones, which show a rapid onset and decay on a subsecond time scale (5, 10, 13), the melanopsin-based intrinsic photoresponse of ipRGCs is relatively insensitive and sluggish, and can persist for tens of seconds up to minutes (5). The kinetics of the melanopsin-based ipRGC photoresponse are directly related to the duration of the phototransduction cascade. Surprisingly, little is known about the termination kinetics of the melanopsin photoresponse, and how these termination kinetics contribute to the multitude of melanopsin-mediated behaviors.

Melanopsin is unique compared with rhodopsin and cone opsins in that it has a long cytoplasmic tail that is predicted to have 38 serines and threonines that are potential phosphorylation sites by GPCR kinase (GRK) (14, 15). Recently, our in vitro studies have revealed that the C terminus phosphorylation is essential for the proper shutoff of the melanopsin light response (14, 15). Similar results have been reported using heterologous expression in Chinese hamster ovary cells and *Xenopus* oocytes (16). Additionally, we showed that light-dependent phosphorylation of melanopsin by GRK occurs in the mouse retina in vivo (14). Finally, a recent study revealed the role of melanopsin C-terminal phosphorylation on the

Significance

Intrinsically photosensitive retinal ganglion cells (ipRGCs) respond to light via both rod/cone-driven synaptic input and intrinsic melanopsin-based phototransduction; however, these two pathways are not functionally redundant. Melanopsin-based phototransduction in ipRGCs is critical for the regulation of the pupillary light reflex (PLR), circadian light responses, masking, and sleep. Therefore, understanding the kinetics and shutoff mechanisms for the melanopsin-based photoresponse will reveal how it contributes to a myriad of behaviors that are controlled by ipRGCs. Here, we show that the melanopsin photoresponse shutoff due to C-terminal phosphorylation determines the kinetics of the intrinsic light response in ipRGCs, the PLR, and reentrainment, but not masking and phase angle of entrainment. These results highlight the elaborate control of how the melanopsin photoresponse regulates vastly different light-mediated behaviors.

Author contributions: P.S., G.R.W., D.C.F., A.G., R.L.B., T.C.B., S.H., and P.R.R. designed research; P.S., G.R.W., D.C.F., C.M.P., M.S.R., A.C.R., and Z.W. performed research; P.S., Z.W., and T.C.B. contributed new reagents/analytic tools; P.S., A.G., C.M.P., L.C., R.L.B., T.C.B., S.H., and P.R.R. analyzed data; and P.S., D.C.F., R.L.B., T.C.B., S.H., and P.R.R. wrote the paper.

The authors declare no conflict of interest.

This article is a PNAS Direct Submission.

[1]To whom correspondence may be addressed. Email: shattar@jhu.edu or probinso@umbc.edu.

[2]Present address: Section on Light and Circadian Rhythms, National Institute of Mental Health, Bethesda, MD 20892.

This article contains supporting information online at www.pnas.org/lookup/suppl/doi:10.1073/pnas.1611893114/-/DCSupplemental.

kinetics of the electrical light response of ipRGCs, but its effects on non–image-forming behaviors remain to be tested (16).

Here, we show that eliminating all of the C-terminal putative phosphorylation sites results in sustained pupil constriction only following high light intensity stimulations. Consistent with the pupillary light reflex (PLR) results, we show that the electrical responses of ipRGCs persist for >15 min from single-cell recordings using patch-clamp electrophysiology. In addition, we find that the lack of GRK-mediated phosphorylation speeds up the reentrainment of animals to a shifted light/dark (L/D) environment but, surprisingly, does not affect masking or the phase angle of entrainment of activity rhythms. These studies suggest that ipRGC subtypes contributing to distinct non–image-forming functions may have different dependencies on GRK-mediated shutoff of the melanopsin photoresponse.

Results

Carboxyl-Terminal Serines and Threonines of Mouse Melanopsin Play a Crucial Role in PLR Kinetics Consistent with Electrophysiological Recordings. Previously, we generated a mutant melanopsin [C-phosphonull (CPΦ); Fig. S1], in which all 38 putative C-terminal GRK phosphorylation sites (serines and threonines) were mutated to alanines and demonstrated that this mutant exhibits delayed deactivation kinetics using an in vitro calcium imaging assay (14, 15) (Fig. S2). A recent paper using multielectrode array (MEA) recordings showed that eliminating nine serines and threonines (S381, S384, T385, T388, S389, S391, S392, S394, and S395) in the C terminus of melanopsin, six of which were shown to be necessary for deactivation kinetics in our in vitro studies (T388, S389, S391, S392, S394, and S395), causes some ipRGCs to exhibit prolonged firing after cessation of the light stimulus (14–16). To investigate the in vivo importance of these phosphorylation sites for melanopsin-mediated behaviors, we expressed C terminus phosphonull melanopsin using adenoassociated virus serotype 2 (AAV2) encoding a Cre-dependent melanopsin and the fluorescent protein mRuby, which was introduced via bilateral intravitreal injections into *Opn4*$^{Cre/Cre}$ mice, a knock-in mouse line in which Cre recombinase replaces melanopsin at the *Opn4* locus (7). Within 2 to 4 wk postinfection, mRuby fluorescence was readily visible in the soma and axons of a population of retinal ganglion cells, and the fluorescence was colocalized by immunofluorescence with virally encoded melanopsin (Fig. S3). Therefore, 4 wk after viral

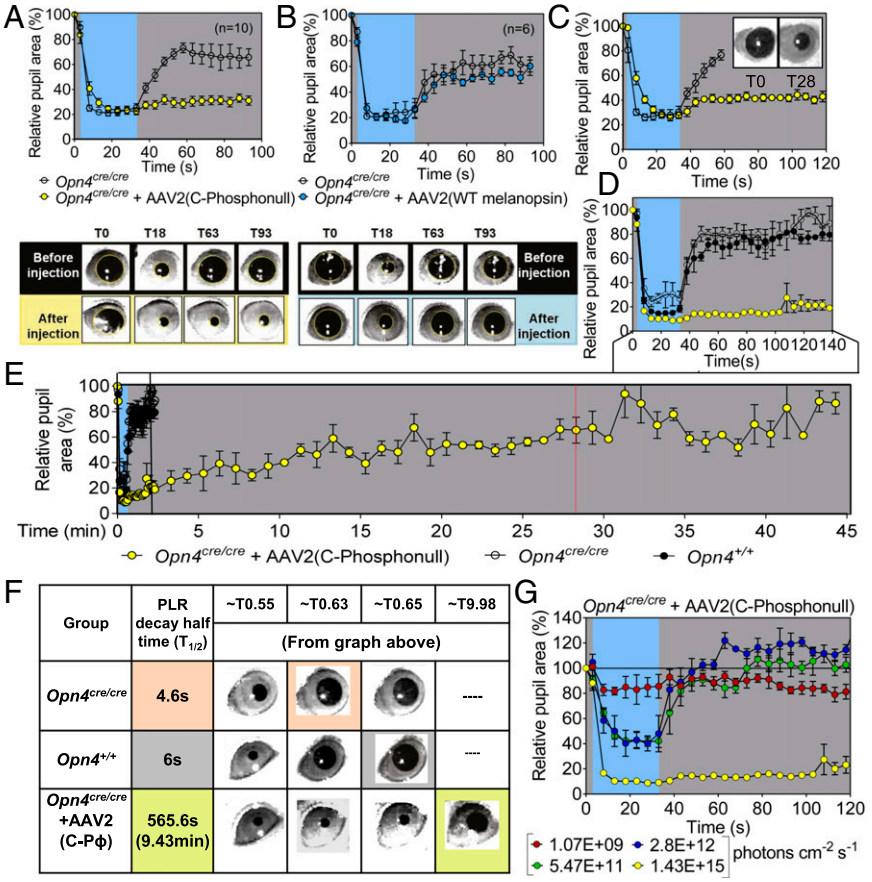

Fig. 1. Expression of melanopsin phosphonull prolongs PLR. The relative pupil area of MKO (*Opn4*$^{Cre/Cre}$), and MKO mice injected with AAV2 virus containing the C-terminal phosphonull melanopsin; AAV2 [mRuby-P2A-phosphonull (CPΦ)-FLAG, simplified to AAV2 (phosphonull)] (*A*, *Top*) and MKO, and MKO mice injected with WT melanopsin AAV2 [mRuby-P2A-melanopsin-FLAG; simplified to AAV2 (melanopsin)] (*B*, *Top*) is shown. Phosphonull-expressing mice (yellow circles; $n = 10$) exhibit prolonged PLR to a high-intensity blue light (~10^{15} photons per $cm^{-2}{\cdot}s^{-1}$), whereas WT melanopsin-expressing mice (blue circles; $n = 6$) are similar to MKO mice [open circles; $n = 16$ ($n = 10$ in *A* and $n = 6$ in *B*)]. (*A* and *B*, *Bottom*) Representative pupil images are shown, with T (time) in seconds. (*C*) Time course for pupil dilation in manually restrained mice after 30 s of blue light (~1.4×10^{15} photons per $cm^{-2}{\cdot}s^{-1}$): phosphonull (yellow circles, $n = 4$) and MKOs (open circles; $n = 4$). (*D* and *E*) Time course as in *C* in restrained mice using a head mount: phosphonull (yellow circles; $n = 3$), MKOs (open circles; $n = 3$), and WT (black solid circles; $n = 3$). The red line demarcates the point at which data are means from three animals; beyond the red line, data are from two animals. (*F*) Table showing $t_{1/2}$ calculations for PLR decay. T0.55 corresponds to 33 s when the light is just turned off. (*G*) Intensity response curves for the phosphonull mice ($n = 3$). Statistical analyses conducted for before and after comparisons in *A* and *B* were linear mixed-effect models between MKO and AAV2 (melanopsin) (not significant, $P = 0.209$) and between MKO and AAV2 (phosphonull) ($P \leq 0.0001$). Statistical analyses in *D* and *E*, using the Kruskal–Wallis test with Dunn's multiple comparisons, were conducted between WT and AAV2 (phosphonull) ($P \leq 0.01$) between MKO and AAV2 (phosphonull) ($P \leq 0.0001$), and between WT and MKO (ns).

infection was chosen as a suitable time point for behavioral assays (17). The viral infection approach allowed us to compare melanopsin-mediated behaviors directly before and after viral infection in the same animal with or without melanopsin expression. $Opn4^{Cre/Cre}$ melanopsin knockout (MKO) mice, where the Cre recombinase replaced the melanopsin gene, exhibited a mean maximum consensual pupil constriction to 22.1% (±1.8 SEM) of the baseline pupil area in response to a high-intensity blue-light stimulus (~$\log_{15}$ photons per $cm^{-2}{\cdot}s^{-1}$) (Fig. 1 *A* and *B*). The PLR for $Opn4^{Cre/Cre}$ mice infected with AAV2 expressing WT melanopsin or C-terminal phosphonull showed no difference in response to the onset of light compared with the knockout animals (Fig. 1 *A* and *B*). After the cessation of the light stimulus however, the pupils of the $Opn4^{Cre/Cre}$ and $Opn4^{Cre/Cre}$ + AAV2 (WT melanopsin) mice dilated within seconds (Fig. 1*B*), whereas the pupils of the $Opn4^{Cre/Cre}$ + AAV2 (C terminus phosphonull) mice exhibited sustained constriction for the remainder of the 60-s recording (Fig. 1*A* and Fig. S4*A*). These results show that C-terminal phosphorylation plays an essential role in the termination of the melanopsin phototransduction pathway, allowing relatively rapid recovery of the dark state after a light stimulus.

In a recently published paper (16), the PLR was also measured in two animals that lack nine C-terminal serines and threonines, and the data suggested persistent pupil constriction up to 60 s after the light was terminated; however, no further time course information about pupil dilation was reported. To examine the full time course of pupil dilation in mice expressing the C terminus phosphonull melanopsin, we used a head-mount setup to record the PLR for up to 45 min. The maximum constriction of MKO animals was attenuated compared with WT animals as shown previously (18), whereas the C-terminal phosphonull animals showed a similar maximum response as observed in WT animals (Fig. 1*D*). Differences in these animals, however, were observed in the pupil dilation phase. Specifically, MKO mice and those mice expressing WT melanopsin exhibited a pupil dilation $t_{1/2}$ of ~6 s and 4.6 s, respectively (Fig. 1 *E* and *F*, Movies S1 and S2, and Fig. S4*B*). In contrast, the pupil of the C terminus phosphonull mice remained constricted 100-fold, with a dilation half-life of ~9.4 min (Fig. 1 *E* and *F*, Movie S3, and Fig. S4*B*). This result reveals that C-terminal phosphorylation of mouse melanopsin is important for its deactivation on a time scale of seconds, and other deactivation mechanisms come into play at later times.

To determine if the longer constriction of the PLR is due to a prolonged light response in the ipRGCs, we carried out single-cell electrophysiology and MEA recordings from ipRGCs expressing virally encoded WT and phosphonull melanopsin. The sensitivity and duration of the WT melanopsin-based light response were consistent with light responses previously reported for endogenous melanopsin (6, 19). A 5-s stimulus of 480-nm light (1×10^{15} photons per $cm^{-1}{\cdot}s^{-1}$) elicited a light-dependent increase in spiking activity (up to 25 Hz) in 18 of 21 mRuby-expressing cells, which typically terminated in <1 min ($t_{1/2}$ = 22 s postpeak, with 90% recovery in 52 s) (Fig. 2 *A* and *B*). In contrast, light responses were much more difficult to detect in ipRGCs expressing the melanopsin C terminus phosphonull. In all, only four of >50 cells that were recorded exhibited a detectable intrinsic light response. The light response in these cells, however, was dramatically prolonged compared with the cells expressing WT melanopsin, showing robust spiking activity persisting for at least for 15 min after the cessation of the light stimulus (Fig. 2 *A* and *B*). In a single cell that remained viable for an extended duration, the firing rate eventually returned to near baseline after more than 20 min. For all of these cells, the light response onset was more sluggish than seen in ipRGCs expressing WT melanopsin, often taking >5 min to reach the peak firing rate (Fig. 2*B*). The peak firing rate was also depressed compared with the peak firing rate of ipRGCs expressing WT melanopsin (Fig. 2*B*). To increase our chances of detecting light-responsive retinal ganglion cells with the phosphonull melanopsin, we performed MEA recordings on retinas expressing either WT or phosphonull melanopsin. In the MEA recordings, ipRGCs expressing WT and phosphonull melanopsin

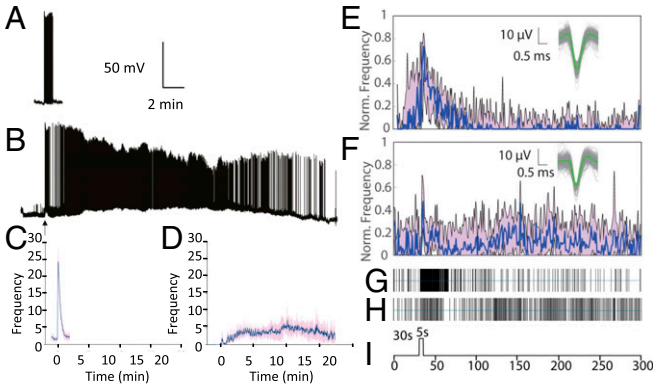

Fig. 2. Phosphonull melanopsin-expressing ipRGCs show a prolonged light response. (*A–D*) Current-clamp recordings from ipRGCs expressing WT (*A*) and phosphonull melanopsin (*B*). Cells were initially maintained at −60 mV. Light stimulation (arrow; 480 nm, 5 s, 1×10^{15} photons per $cm^{-2}{\cdot}s^{-1}$) increased action potential frequency, which terminated within 1 min in WT but was prolonged (>20 min) for phosphonull melanopsin. Spike frequency (averaged over 2-s bins) is shown as a function of time in ipRGCs expressing WT (*C*; n = 10) and phosphonull (*D*; n = 4); error bars are SEM. (*E–I*) MEA recordings of retinas from WT or AAV2 (phosphonull). Normalized frequency response curves to a 5-s blue-light pulse (digitized in *I*) of nine (*E*, WT) and 11 (*F*, phosphonull) ipRGCs are shown. Data (binned to 1-s bins and normalized to the maximum firing frequency) are represented as the median (blue curve) and 25–75% interquartile interval (purple area). Maximum frequency ranged from 8 to 39 Hz for WT and from 10–48 Hz for ipRGCs. WT ipRGCs return to baseline at about 60 s after the 5-s light pulse, whereas phosphonull ipRGCs continue to fire at a reduced and inconsistent rate for the whole length of this recording (4 min and 25 s after the light is turned off). Example spike raster plots for individual light responsive units for WT (*G*) and phosphonull (*H*) ipRGCs (n = 4 for WT and n = 3 for phosphonull) are shown. Registered, overlaid spikes (gray curves) for the individual cells in *G* and *H* are shown in *E* and *F* (*Insets*), together with their respective average spikes (green line). (*I*) Digital synchronized signal shows the experimental protocol.

were detected in approximately equal numbers (about 5% of all identified cells), and, typically, several ipRGCs were detected in each retinal preparation. We found that for the MEA recordings from WT animals, the majority of ipRGCs shut off within 50 s after the light stimulation. In contrast, for the phosphonull animals, ipRGC responses persist for at least 4.5 min, which is the longest recording time (Fig. 2*C*). Together, the single-cell data and the MEA recordings show that the persistent light response in ipRGCs is consistent with the persistence response of the PLR in darkness.

To determine if the longer pupil dilation times are specific to melanopsin-based phototransduction and not to rod/cone input (18, 20), we measured the PLR at four different light intensities to generate intensity response curves. As expected, the dilation phase of the PLR did not show any difference between $Opn4^{Cre/Cre}$ + AAV2 (C terminus phosphonull) and $Opn4^{Cre/Cre}$ at low light intensities, where the PLR is driven by rod/cone input (18, 20) (Fig. 1*G* and Fig. S5). At intensities >15 log (photons per $cm^{-2}{\cdot}s^{-1}$), however, which is known to activate melanopsin-based phototransduction (18, 19), the curve for $Opn4^{Cre/Cre}$ + AAV2 (C terminus phosphonull) deviated from $Opn4^{Cre/Cre}$ and WT animals (Fig. 1*G* and Fig. S5). This result demonstrates that GRK-based shutoff of melanopsin-based phototransduction through C-terminal phosphorylation is important for the proper kinetic regulation of the PLR.

The Delayed Shutoff Properties of the C Terminus Melanopsin Phosphonull Mutant Renders Phase Delays More Efficient but, Surprisingly, Does Not Affect the Phase Angle of Entrainment. To determine if C-terminal phosphorylation of melanopsin plays a role in circadian photoentrainment, we placed animals under a 16-h/8-h (16:8) L/D cycle before and after injections with AAV2 (WT melanopsin) or AAV2 (C terminus phosphonull). $Opn4^{Cre/Cre}$ mice were able to

NEUROSCIENCE

photoentrain to 16:8 L/D due to the presence of intact rods and cones (Fig. 3*A*, *Top* and *B*, *Top*), and *Opn4*$^{Cre/Cre}$ mice infected with WT melanopsin also showed photoentrainment as expected (Fig. 3*A*, *Bottom*). Based on our PLR data, we expected that exposing the *Opn4*$^{Cre/Cre}$ mice infected with C terminus phosphonull melanopsin to 16 h of light would cause these animals to have a severely delayed phase angle of entrainment, because only 5 s of light stimulation leads to more than 15 min of melanopsin-based spiking activity. Surprisingly, we failed to see any changes in the phase angle of entrainment in these animals (Fig. 3*F*). This result indicates that after prolonged light stimulation, shutoff mechanisms independent of GRK-mediated C-terminal phosphorylation contribute to melanopsin phototransduction termination even in the presence of light input.

To investigate the ability of the animals to reentrain to a shifted L/D cycle, we delayed the dark onset by 6 h, mimicking a transmeridian flight from Amsterdam to New York, in *Opn4*$^{Cre/Cre}$ mice to 16:8 L/D before and after injections with AAV2 (WT melanopsin) and AAV2 (C terminus phosphonull). Before viral injections, *Opn4*$^{Cre/Cre}$ mice took an average of 9 d (±0.85 SEM) to shift their activities and entrain to the delayed L/D cycle (Fig. 3 *A* and *B*, *Top* and *C* and *D*, *Left*). *Opn4*$^{Cre/Cre}$ + AAV2 (WT melanopsin), on average, needed 5.6 d (±0.68 SEM) to shift their activities (Fig. 3*A*, *Bottom* and *C*, *Right*), whereas *Opn4*$^{Cre/Cre}$ + AAV2 (C terminus phosphonull) needed only an average of 2.8 d (±0.79 SEM) (Fig. 3*B*, *Bottom* and *D*, *Right*). The days needed to photoentrain for the infected animals were significantly different from the days needed for their uninfected counterparts (Fig. 3 *C* and *D*). The

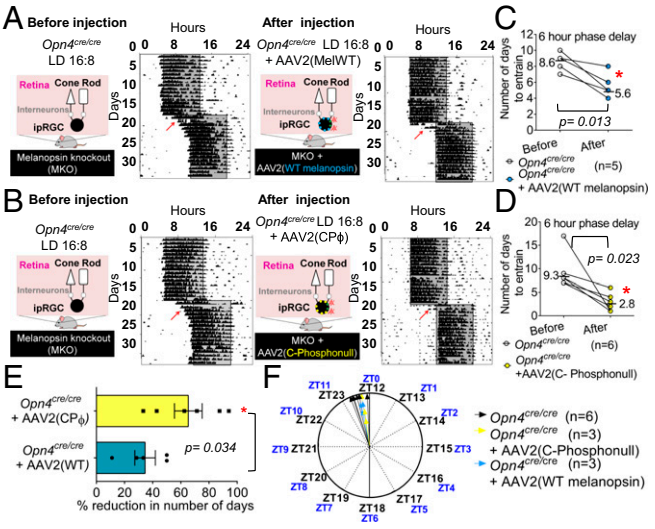

Fig. 3. Phosphonull and WT melanopsin rescue the jet-lag deficit observed in MKO mice. (*A*) Graphical depiction and representative actograms using a paradigm of a 16:8 L/D cycle of one MKO before (*Top*) and after (*Bottom*) injection with AAV2 (melanopsin; red particles are virus). MelWT, melanopsin WT. (*B*) Same as in *A*, but now with AAV2 (phosphonull). Red arrows indicate the 6-h jet lag. (*C*) Number of days for reentrainment: MKO before and after injection with AAV2 (phosphonull; $n = 6$). (*D*) Number of days for reentrainment with AAV2 (melanopsin). (*E*) Percent reduction in number of days taken by MKOs to reentrain after injection with either AAV2 (melanopsin; blue) or AAV2 (phosphonull; yellow). (*F*) Comparison of phase angle of entrainment for MKO (black, $n = 6$), AAV2 (melanopsin; blue, $n = 3$) and AAV2 (phosphonull; yellow, $n = 3$). Statistical analyses conducted in *C* and *D* for before and after comparisons were paired two-tailed *t* tests comparing MKO and AAV2 (melanopsin; $P = 0.013$) and MKO and AAV2 (phosphonull; $P = 0.023$) (*$P \leq 0.05$). The comparison between AAV2 (melanopsin) and AAV2 (phosphonull) in *E* was conducted by an unpaired *t* test with Welch's correction test ($P = 0.034$) (*$P \leq 0.05$). Statistical analyses for *F* were paired two-tailed *t* tests comparing MKO and AAV2 [melanopsin; not significant (ns), $P = 0.388$] and MKO AAV2 (phosphonull; ns, $P = 0.47$). A comparison between the three groups was conducted by the Kruskal–Wallis test (ns, $P = 0.150$).

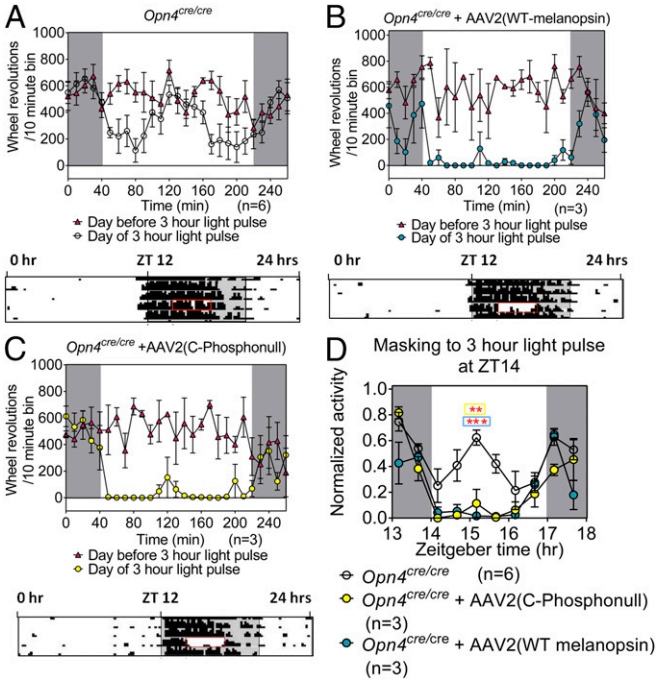

Fig. 4. Both WT and phosphonull melanopsin rescue the masking deficit in MKO. A comparison of wheel-running activities recorded in 10-min bouts between the day before and day of a 3-h light pulse in MKO (*A*), AAV2 (melanopsin) (*B*), and AAV2 (phosphonull) (*C*) is shown. A 3-h light pulse initiated at Zeitgeber time 14 (ZT14) is indicated by the red box. (*D*) Comparison of the normalized activities of the three groups represented in 20-min bins from ZT13 to ZT18. Wheel revolutions were normalized to the highest bout, which occurs outside of the window of time shown here. Statistical analyses conducted in *A*–*C* for before and after comparisons were linear mixed-effect models comparing activities on the day before and day of a 3-h light pulse in MKO ($P = 0.042$), AAV2 (melanopsin; $P = 0.009$), and AAV2 (phosphonull; $P = 0.045$). Comparison of the three groups in *D* was conducted by two-way ANOVA with multiple comparisons (**$P \leq 0.01$, ***$P \leq 0.001$).

presence of melanopsin (WT or C terminus phosphonull) renders *Opn4*$^{Cre/Cre}$ mice more efficient in reentraining to phase delays (Fig. 3 *A* and *B*).

Opn4$^{Cre/Cre}$ + AAV2 (C terminus phosphonull) mice exhibited a 65.3% (±9.8 SEM) reduction in the number of days taken to reentrain in comparison to *Opn4*$^{Cre/Cre}$ mice (Fig. 3*E*). Similarly, *Opn4*$^{Cre/Cre}$ + AAV2 (WT melanopsin) mice exhibited a 34.6% (±7.3 SEM) reduction in the number of days taken to reentrain in comparison to *Opn4*$^{Cre/Cre}$ mice (Fig. 3*E*). The reduction of days needed for reentrainment in the phosphonull mice was significantly different from WT melanopsin mice.

Both WT and C Terminus Phosphonull Melanopsin Rescue Negative Masking Deficit in MKO. In addition to circadian photoentrainment, masking is another mechanism by which animals exhibit light-mediated changes in behavior (21). Nocturnal animals reduce their activity during their subjective night when exposed to a high-intensity light stimulus. MKO animals exhibit a deficit in negative masking at high light intensities (21) (Fig. 4*A*). *Opn4*$^{Cre/Cre}$ mice were housed in a 16:8 L/D cycle and given a 3-h light pulse (500 lux) at Zeitgeber time 14 (ZT14) (2 h after the onset of darkness). When *Opn4*$^{Cre/Cre}$ mice were injected with either AAV2 (WT melanopsin) or AAV2 (C terminus phosphonull), a rescue of this deficit was observed (Fig. 4 *B* and *C*). There was no apparent difference in the persistence of the masking response after the cessation of the light stimulus between either melanopsin construct (Fig. 4*D*). In fact, similar to the phase angle of entrainment, the masking response is similar between melanopsin and C terminus phosphonull (Figs. 3*F* and 4*D*).

Discussion

We used AAV2 viral expression of melanopsin and the C terminus phosphonull form of melanopsin to study the effect of restoration of intrinsic light responses on MKO animals at adult stages. GPCRs commonly undergo deactivation/desensitization through light-dependent phosphorylation of multiple C-terminal serine and threonine residues by GRKs, and subsequent arrestin-mediated termination of receptor signaling (22). Studies on rhodopsin indicate that multiple phosphorylations in the C terminus are required for complete quenching of the rhodopsin-mediated light response in rod photoreceptors (23). Surprisingly, the significance of melanopsin's C terminus phosphorylation in ipRGC function has been a subject of debate in the field (24–26). This controversy arose from the observation that the shutoff of melanopsin phototransduction is prolonged and variable after the cessation of light stimulation. A recent paper in which the authors used MEA recordings from retinas infected with melanopsin lacking the six serines and threonines (T388, S389, S391, S392, S394, and S395) that we reported earlier (14, 15), plus three additional serines and threonines (S381, S384, and T385), showed that melanopsin deactivation is important in vivo (16). In this study, we determine the role of C terminus phosphorylation of melanopsin for several light-dependent behaviors and demonstrate that C-terminal phosphorylation is essential for the regulation of PLR and phase delay, but not masking behavior or the phase angle of entrainment.

We found that even in the absence of all of the C terminus phosphorylation sites, the PLR eventually returns to baseline in minutes. This finding suggests that alternative shutoff mechanisms are involved in terminating the melanopsin phototransduction pathway. The slow termination responses of phosphonull melanopsin mutant-expressing ipRGCs, however, did not affect the phase angle of entrainment, but did cause faster reentrainment in response to a jet-lag paradigm. These results highlight the exciting finding that the C terminus contribution to melanopsin function is dependent on both behavior and light duration.

Although C-terminal phosphorylation sites are crucial for normal deactivation of melanopsin, we do not know precisely the candidate GRK involved in this function. GRK1–GRK6 are expressed in the retina, and GRK2, GRK3, and GRK5 are known to be expressed in ipRGCs (14). We demonstrated that GRK2 and GRK3 are coimmunoprecipitated with melanopsin in ipRGCs in a light-dependent manner (14). Despite this evidence that suggests an interaction between GRKs and melanopsin, it has been shown that GRK2 regulates melanopsin activity only minimally, and only in very young animals (25). It was demonstrated that genetic deletion of GRK2 does not significantly impact melanopsin activity or ipRGC function in adult animals (25). We propose that the lack of phenotype in adult animals could be explained by the presence of other GRKs in ipRGCs (25). In the absence of GRK2, melanopsin could be phosphorylated by GRK3, thereby compensating for the loss of GRK2. Further studies that completely ablate all GRKs in a conditional manner may shed light on the identity of the GRK primarily phosphorylating melanopsin in native conditions. Melanopsin is a promiscuous GPCR in terms of its interaction partners; it associates with more than one type of G protein (27–29). Similarly, it is likely that melanopsin is nonselective in the association of GRK type.

Our PLR data are consistent with both single-cell and MEA recordings. We observed, however, that for single-cell recordings, very few cells were light-responsive in the C terminus phosphonull retinas. We suggest that the lack of responsivity is caused by exposure to 540-nm light, which is required to locate virally infected cells expressing mRuby. This 540-nm light is capable of activating melanopsin phototransduction, which we suspect causes the light response of the ipRGCs to become saturated. Consistent with this explanation, we observed that ipRGCs from WT-infected animals had a resting membrane potential of −54 mV (±7.5 SEM), whereas ipRGCs from phosphonull-infected animals had a resting membrane potential of −46 mV (±3.5 SEM). Furthermore, when we used MEA recordings, in which ipRGCs do not need to be located and retinas are prepared in darkness, we were able to detect more light-responsive ipRGCs in the C terminus phosphonull retinas. However, similar to single-cell recordings, the ipRGCs in these C terminus phosphonull retinas showed reduced responses to light onset. One possibility is that prolonged signaling of the C-terminal phosphonull melanopsin may result in down-regulation of components of the phototransduction cascade.

How can we reconcile the differences in the contribution and duration of the C terminus phosphorylation to the variety of the melanopsin-based behavioral light responses? The most logical possibility is that different ipRGC subtypes (7) use distinct shutoff mechanisms due to differential expression of GRKs, for example. Because ipRGC subtypes contribute to different behaviors (4, 6, 7, 21), the importance of the shutoff response is going to depend on which subtype is driving a specific behavior. Another possibility is pigment regeneration in the dark after light exposure. For example, in the PLR, after the light is turned off, the pupil eventually fully dilates to baseline levels. This finding indicates that a pathway independent of C terminus phosphorylation can function in the dark to restore melanopsin close to the basal state. Such a pathway could include the dissociation of the chromophore from melanopsin, followed by regeneration of the inactive form due to the rebinding of the *cis* form of the chromophore. This explanation is consistent with the idea that melanopsin seems to return to the basal state under dark conditions (30). It is important to highlight that a similar phenomenon is observed in rod photoreceptors lacking rhodopsin kinase, where although the light response is prolonged, it does deactivate using an alternate deactivation mechanism described by a single exponential function and a time constant of 3 s (31).

A surprising outcome of this study is that in CPϕ animals, even after 16 h of light stimulation, the phase angle of entrainment was similar and masking responses were indistinguishable from masking responses in animals expressing WT melanopsin. What are the possible mechanisms for such an effect? It is hard to come up with a totally satisfying answer to this question; however, we advance three different possibilities: (*i*) Melanopsin is an R-type opsin and is either a bistable or tristable visual pigment; therefore, under continuous light stimulation, photoisomerization could revert some active melanopsin back to the basal state (16, 26); (*ii*) different ipRGC subtypes use distinct shutoff mechanisms for the ipRGC responses, with some subtypes using a GRK-independent pathway; and (*iii*) under prolonged light stimulations, shutoff mechanisms involving components of the phototransduction pathway downstream of the melanopsin pigment are involved in terminating the response. Regardless of the reason for these differences, our study has just scratched the surface for the complexity of the shutoff responses in ipRGCs. In addition, we have demonstrated that light-activated phosphorylation of melanopsin's C terminus is an important posttranslational modification regulating the lifetime of active melanopsin for regulating the PLR and the speed of reentrainment.

Methods

Physiological and Behavioral Analyses of Animals. All experiments were conducted in accordance with NIH guidelines and were approved by the institutional care and use committee of the universities involved. All protocols were in accordance with The Johns Hopkins University Animal Care and Use Committee guidelines. All procedures for patch-clamp recordings were carried out in compliance with Washington State University's Institutional Animal Care and Use Committee guidelines. We used physiological tests to determine the photoresponse of ipRGCs using MEA recordings (30–34)* and single-cell patch-clamp recordings (35). We used behavioral tests to determine the wheel-running activity of the animals (36, 37), PLR (18, 20), phase shifting and phase angle of entrainment (36, 37), and direct effects of light on activity (21).

*Ghahari A, Badea TC, 38th Annual International Conference of the IEEE Engineering in Medicine and Biology Society, August 16–20, 2016, Orlando, FL.

ACKNOWLEDGMENTS. We thank Joe Blasic, William Keenan, Evan Cameron, and all others members of the P.R.R. and S.H. laboratories for their helpful comments; Beverly Wu for the viral vector backbone; and Hiryanna Suja for technical assistance with vector packaging. This study was supported by NIH Grants R01EY019053 (to P.R.R.), GM076430 (to S.H.), and EY024452 (to S.H.); a grant from the Chapman–Perelman NeuroPsychoAnalytic Society (to R.L.B.); and a grant from the National Eye Institute Intramural Research Program (to T.C.B.).

1. Provencio I, Jiang G, De Grip WJ, Hayes WP, Rollag MD (1998) Melanopsin: An opsin in melanophores, brain, and eye. *Proc Natl Acad Sci USA* 95(1):340–345.
2. Güler AD, et al. (2008) Melanopsin cells are the principal conduits for rod-cone input to non-image-forming vision. *Nature* 453(7191):102–105.
3. Porter ML, et al. (2012) Shedding new light on opsin evolution. *Proc Biol Sci* 279(1726): 3–14.
4. Hattar S, et al. (2003) Melanopsin and rod-cone photoreceptive systems account for all major accessory visual functions in mice. *Nature* 424(6944):76–81.
5. Panda S, et al. (2003) Melanopsin is required for non-image-forming photic responses in blind mice. *Science* 301(5632):525–527.
6. Berson DM, Dunn FA, Takao M (2002) Phototransduction by retinal ganglion cells that set the circadian clock. *Science* 295(5557):1070–1073.
7. Ecker JL, et al. (2010) Melanopsin-expressing retinal ganglion-cell photoreceptors: Cellular diversity and role in pattern vision. *Neuron* 67(1):49–60.
8. Schmidt TM, Taniguchi K, Kofuji P (2008) Intrinsic and extrinsic light responses in melanopsin-expressing ganglion cells during mouse development. *J Neurophysiol* 100(1):371–384.
9. Schmidt TM, Kofuji P (2009) Functional and morphological differences among intrinsically photosensitive retinal ganglion cells. *J Neurosci* 29(2):476–482.
10. Wong KY, Dunn FA, Graham DM, Berson DM (2007) Synaptic influences on rat ganglion-cell photoreceptors. *J Physiol* 582(Pt 1):279–296.
11. Dacey DM, et al. (2005) Melanopsin-expressing ganglion cells in primate retina signal colour and irradiance and project to the LGN. *Nature* 433(7027):749–754.
12. Perez-Leon JA, Warren EJ, Allen CN, Robinson DW, Brown RL (2006) Synaptic inputs to retinal ganglion cells that set the circadian clock. *Eur J Neurosci* 24(4):1117–1123.
13. Arshavsky VY, Lamb TD, Pugh EN, Jr (2002) G proteins and phototransduction. *Annu Rev Physiol* 64:153–187.
14. Blasic JR, Jr, Brown RL, Robinson PR (2012) Light-dependent phosphorylation of the carboxy tail of mouse melanopsin. *Cell Mol Life Sci* 69(9):1551–1562.
15. Blasic JR, Jr, et al. (2014) Identification of critical phosphorylation sites on the carboxy tail of melanopsin. *Biochemistry* 53(16):2644–2649.
16. Mure LSS, et al. (2016) Melanopsin-encoded response properties of intrinsically photosensitive retinal ganglion cells. *Neuron* 90(5):1016–1027.
17. Lin B, Koizumi A, Tanaka N, Panda S, Masland RH (2008) Restoration of visual function in retinal degeneration mice by ectopic expression of melanopsin. *Proc Natl Acad Sci USA* 105(41):16009–16014.
18. Lucas RJ, et al. (2003) Diminished pupillary light reflex at high irradiances in melanopsin-knockout mice. *Science* 299(5604):245–247.
19. Do MT, et al. (2009) Photon capture and signalling by melanopsin retinal ganglion cells. *Nature* 457(7227):281–287.
20. Lucas RJ, Douglas RH, Foster RG (2001) Characterization of an ocular photopigment capable of driving pupillary constriction in mice. *Nat Neurosci* 4(6):621–626.
21. Mrosovsky N, Hattar S (2003) Impaired masking responses to light in melanopsin-knockout mice. *Chronobiol Int* 20(6):989–999.
22. Shukla AK, Xiao K, Lefkowitz RJ (2011) Emerging paradigms of β-arrestin-dependent seven transmembrane receptor signaling. *Trends Biochem Sci* 36(9):457–469.
23. Mendez A, et al. (2000) Rapid and reproducible deactivation of rhodopsin requires multiple phosphorylation sites. *Neuron* 28(1):153–164.
24. Do MT, Yau KW (2013) Adaptation to steady light by intrinsically photosensitive retinal ganglion cells. *Proc Natl Acad Sci USA* 110(18):7470–7475.
25. Sexton TJ, Van Gelder RN (2015) G-protein coupled receptor kinase 2 minimally regulates melanopsin activity in intrinsically photosensitive retinal ganglion cells. *PLoS One* 10(6):e0128690.
26. Emanuel AJ, Do MT (2015) Melanopsin tristability for sustained and broadband phototransduction. *Neuron* 85(5):1043–1055.
27. Newman LA, Walker MT, Brown RL, Cronin TW, Robinson PR (2003) Melanopsin forms a functional short-wavelength photopigment. *Biochemistry* 42(44):12734–12738.
28. Walker MT, Brown RL, Cronin TW, Robinson PR (2008) Photochemistry of retinal chromophore in mouse melanopsin. *Proc Natl Acad Sci USA* 105(26):8861–8865.
29. Chew KS, Schmidt TM, Rupp AC, Kofuji P, Trimarchi JM (2014) Loss of gq/11 genes does not abolish melanopsin phototransduction. *PLoS One* 9(5):e98356.
30. Wong KY, Dunn FA, Berson DM (2005) Photoreceptor adaptation in intrinsically photosensitive retinal ganglion cells. *Neuron* 48(6):1001–1010.
31. Chen CK, et al. (1999) Abnormal photoresponses and light-induced apoptosis in rods lacking rhodopsin kinase. *Proc Natl Acad Sci USA* 96(7):3718–3722.
32. Cahill H, Nathans J (2008) The optokinetic reflex as a tool for quantitative analyses of nervous system function in mice: Application to genetic and drug-induced variation. *PLoS One* 3(4):e2055.
33. Matsuoka RL, et al. (2011) Class 5 transmembrane semaphorins control selective Mammalian retinal lamination and function. *Neuron* 71(3):460–473.
34. Ye X, et al. (2009) Norrin, frizzled-4, and Lrp5 signaling in endothelial cells controls a genetic program for retinal vascularization. *Cell* 139(2):285–298.
35. Warren EJ, Allen CN, Brown RL, Robinson DW (2003) Intrinsic light responses of retinal ganglion cells projecting to the circadian system. *Eur J Neurosci* 17(9):1727–1735.
36. Panda S, et al. (2002) Melanopsin (Opn4) requirement for normal light-induced circadian phase shifting. *Science* 298(5601):2213–2216.
37. Ruby NF, et al. (2002) Role of melanopsin in circadian responses to light. *Science* 298(5601):2211–2213.
38. Kredel S, et al. (2009) mRuby, a bright monomeric red fluorescent protein for labeling of subcellular structures. *PLoS One* 4(2):e4391.
39. Kim JH, et al. (2011) High cleavage efficiency of a 2A peptide derived from porcine teschovirus-1 in human cell lines, zebrafish and mice. *PLoS One* 6(4):e18556.
40. Ye X, et al. (2003) Norrin, frizzled-4, and Lrp5 signaling in endothelial cells controls a genetic program for retinal vascularization. *Neuron* 4(5):949–956.
41. Grant CA, Ponnazhagan S, Wang XS, Srivastava A, Li T (1997) Evaluation of recombinant adeno-associated virus as a gene transfer vector for the retina. *Curr Eye Res* 16(9):949–956.
42. Gooley JJ, Lu J, Fischer D, Saper CB (2003) A broad role for melanopsin in nonvisual photoreception. *J Neurosci* 23(18):7093–7106.